Electronic Supplementary Material (ESI) for Green Chemistry.
This journal is © The Royal Society of Chemistry 2016

Supplementary Information

Effective Recycling of Manganese Oxide Cathodes for Lithium Based Batteries

Authors: Altug S. Poyraz,[a] Jianping Huang,[b] Shaobo Cheng,[a,c] David C. Bock,[a] Lijun Wu,[a] Yimei Zhu,[a] Amy C. Marschilok[b,d*], Kenneth J. Takeuchi[b,d*], and Esther S. Takeuchi[a,b,d*]

Affiliations:

[a] Energy Sciences Directorate, Brookhaven National Laboratory, Upton, NY 11973, USA
[b] Department of Chemistry, Stony Brook University, Stony Brook, NY 11794, USA.
[c] Department of Materials Science and Engineering, Tsinghua University, Beijing, 100084, China
[d] Department of Materials Science and Engineering, Stony Brook University, Stony Brook, NY 11794, USA
* Corresponding Authors: (ACM) amy.marschilok@stonybrook.edu, (KJT) kenneth.takeuchi.1@stonybrook.edu, (EST) esther.takeuchi@stonybrook.edu

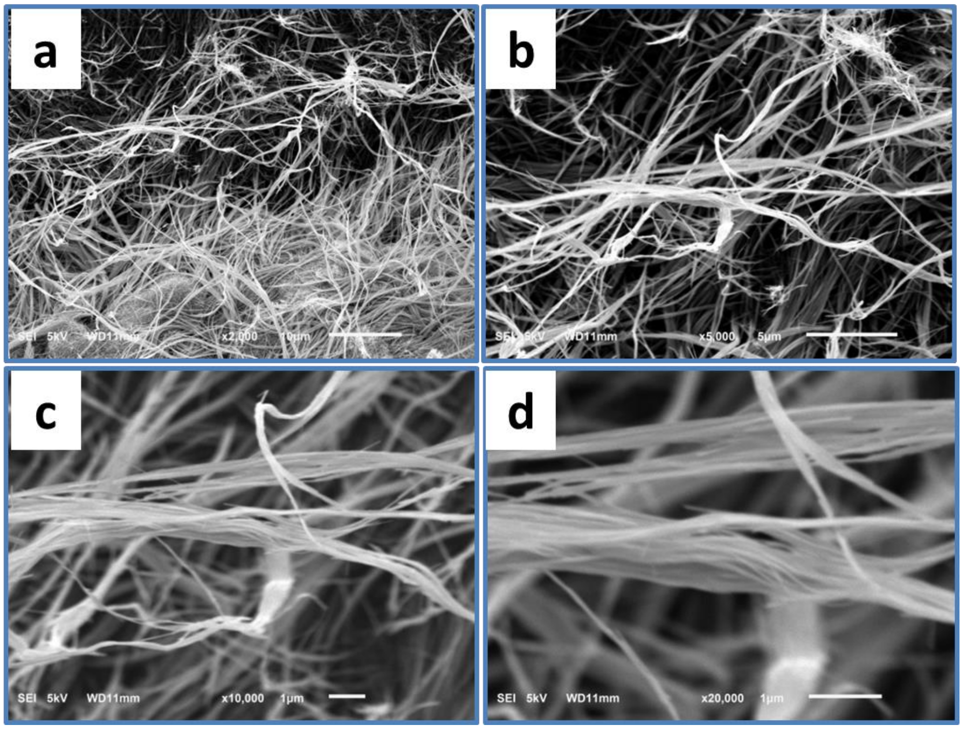

Fig. S1 Morphology of manganese oxide (OMS-2) electroactive material. SEM images of a OMS-2 material with different magnifications: **(a)** 2kx, scale bar 10μm. **(b)** 5kx, scale bar 5μm. **(c)** 10kx, scale bar 1μm. **(d)** 20kx, scale bar 1μm.

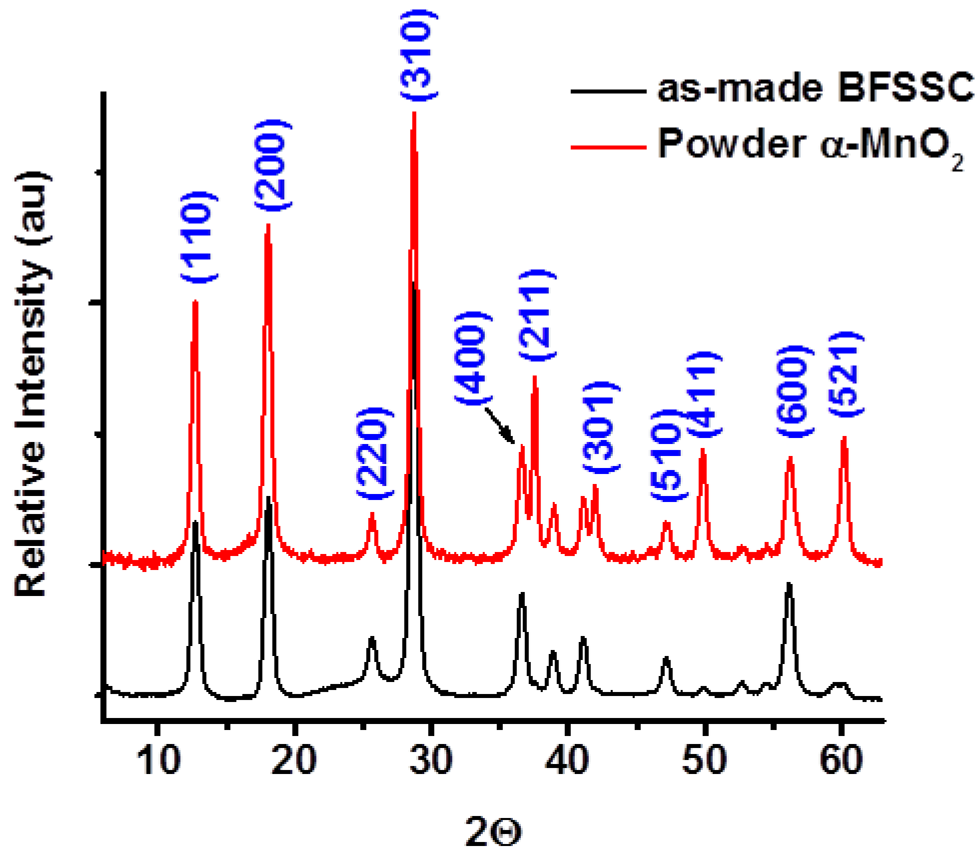

Fig. S2 Diffraction pattern comparison. X-ray Diffraction (XRD) patterns of as-made grounded OMS-2 (Powder α-MnO_2) and binder free self-supporting cathode binder-free self-supporting cathode (BFSSC) (83wt. % OMS-2) materials. ($K_xMn_8O_{16}$, JCPDS 029-1020)

As-made BFSSC has higher relative intensities for (hk0) diffraction lines compared to to (00l) lines. (hk0) crystallographic planes are parallel to the 2x2 tunnels. Therefore, higher intensities of (hk0) lines are likely due to preferential orientation of the nanofibers in their preferred crystal growth direction (c-axis)[1, 2]. On the other hand, after grounding OMS-2 nanofibers (Powder α-MnO_2), (00l) diffraction lines becomes more prominent in the pattern. Yuan et al. also reported preferred orientations for OMS-2 fibers and OMS-2 tetragonal prisms both prepared with similar hydrothermal methods[3, 4].

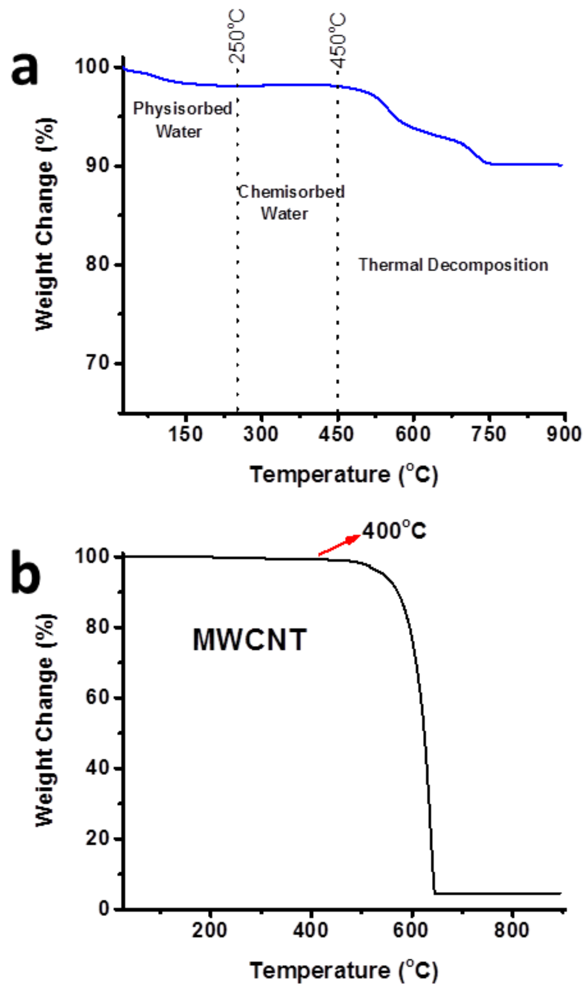

Fig. S3 Thermal stability and water content of OMS-2 and MWCNT**. a)** Thermal Gravimetric Analysis (TGA) profile of OMS-2 (α-MnO_2). The TGA graph is split into three parts, separated by dashed lines, physisorbed water (RT- 250°C), Structural (Tunnel) Water (250 - ~450°C), and O_2 evolution (thermal decomposition) (>450°C). **b)** TGA profile of multiwall carbon nanotube (MWCNT).

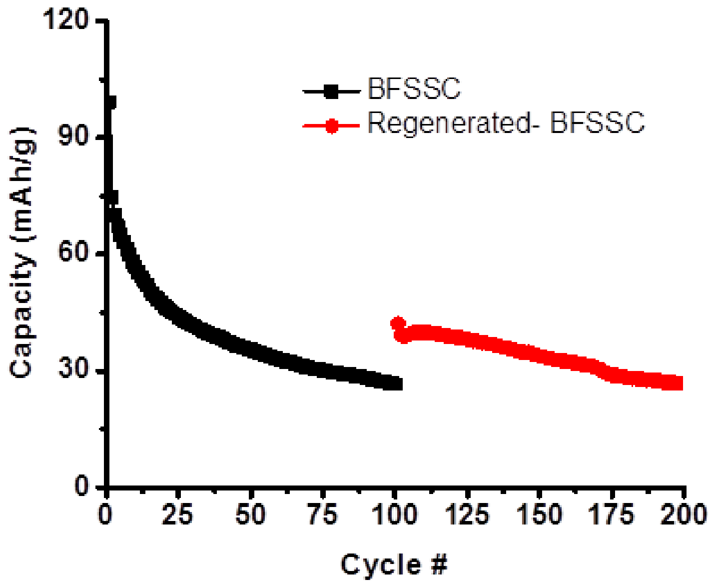

Fig. S4 Regeneration Control experiment**.** Galvanostatic cycling performance of BFSSC regenerated by only rinsing with DMC and dried at RT in a vacuum oven (No heating). Current density was 50mA/g (2.0 and 3.9 V vs. Li/Li^+).

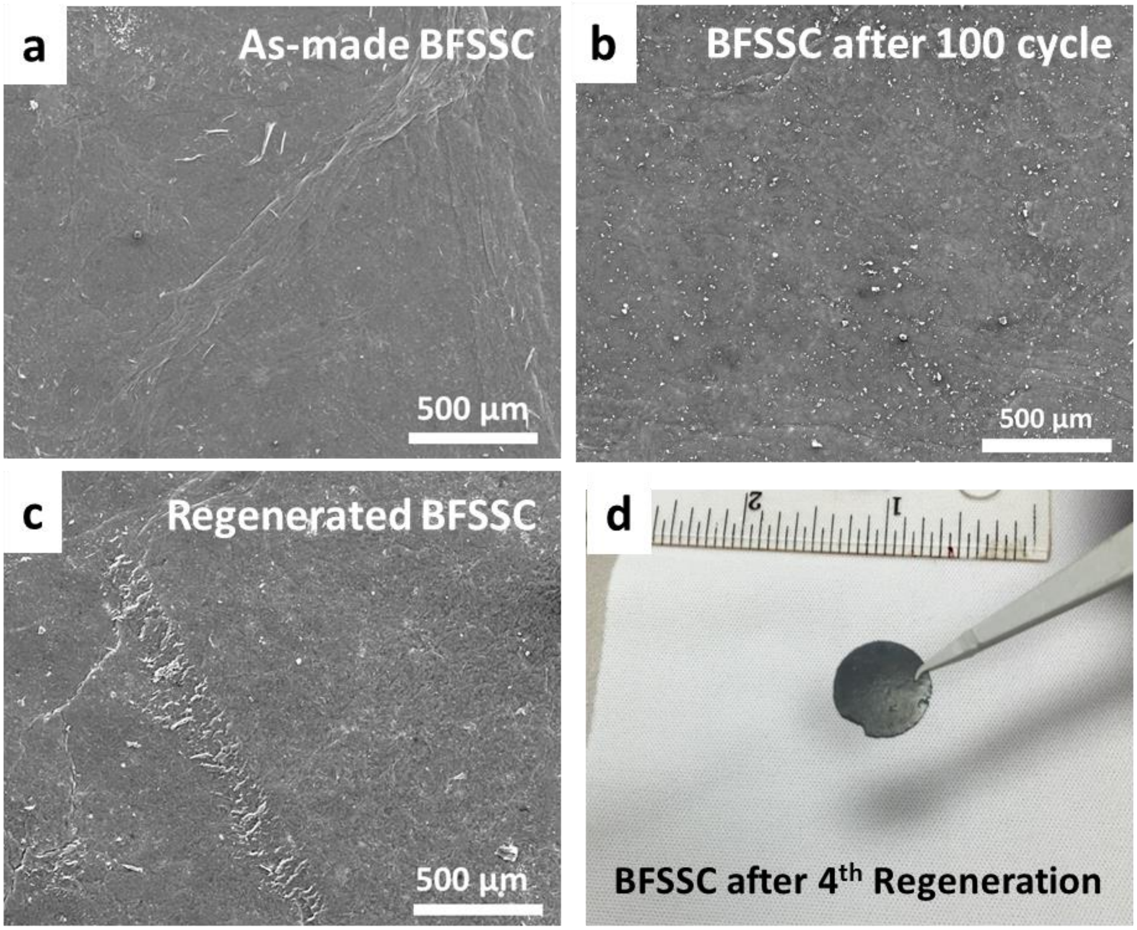

Fig. S5 SEM images showing the macro structure of (**a**) as-made binder free self-supporting cathode (BFSSC), (**b**) The BFSSC sample cycled for 100 times, (**c**) The BFSSC sample cycled for 300 times and (**d**) optical image of BFSSC sample after 4th regeneration.

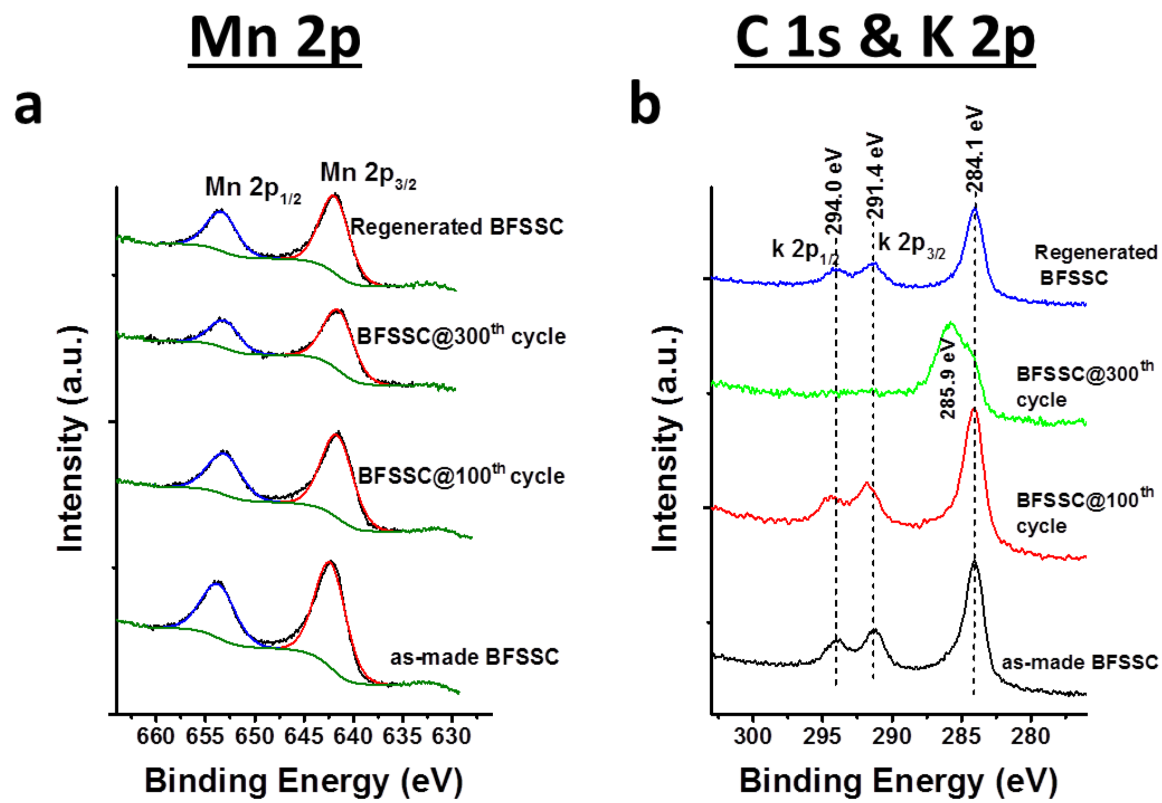

Fig. S6 Structural changes of manganese and carbon during the cathode regeneration. X-ray Photoelectron spectra (XPS) of as-made BFSSC, BFSSCs galavanostatically cycled for 100 (BFSSC@100th cycle) and 300 (BFSSC@300th cycle) times with 50mA/g rate, and regenerated BFSSC after 100 cycles. (**a**) Mn 2p and (**b**) C1s and K2p spectral regions.

Upon battery cycling, a new C1s peak appeared at around ~285.9 eV after 300 cycles (BFSSC@300th cycle), (**Fig. S7a**). We attributed the new C1s peak to polymeric species (i.e. polyethers or poly carbonates) formed by electrolyte oxidation on the high voltage manganese oxide cathode[5-7]. However, no change at O_{ads} and C1s was observed after 100 cycles, suggesting a slow SEI formation rate in the studied voltage window (2.0 - 3.9 V) or partial removal of SEI by DMC rinsing. Another notable change in the XPS analyses was the decrease of the K2p peak intensities during battery cycling (**Fig. S7b**). K2p peak intensities gradually decreased and no K2p peaks were observed after 300 cycles. Lower K2p peak intensities indicate a decrease at the potassium content during the battery cycling. The decrease at the potassium content can be attributed to the deinsertion of potassium during the charging step[8, 9].

Table S1: XPS Mn2p of as-made, cycled, and regenerated BFSSCs

Sample	Mn 2p (eV)	
	2p $_{1/2}$	**2p $_{3/2}$**
As-made BFSSC	653.7	642.4
BFSSC@100th cycle	653.1	641.6
BFSSC@300th cycle	653.1	641.5
Regenerated BFSSC	653.5	641.9

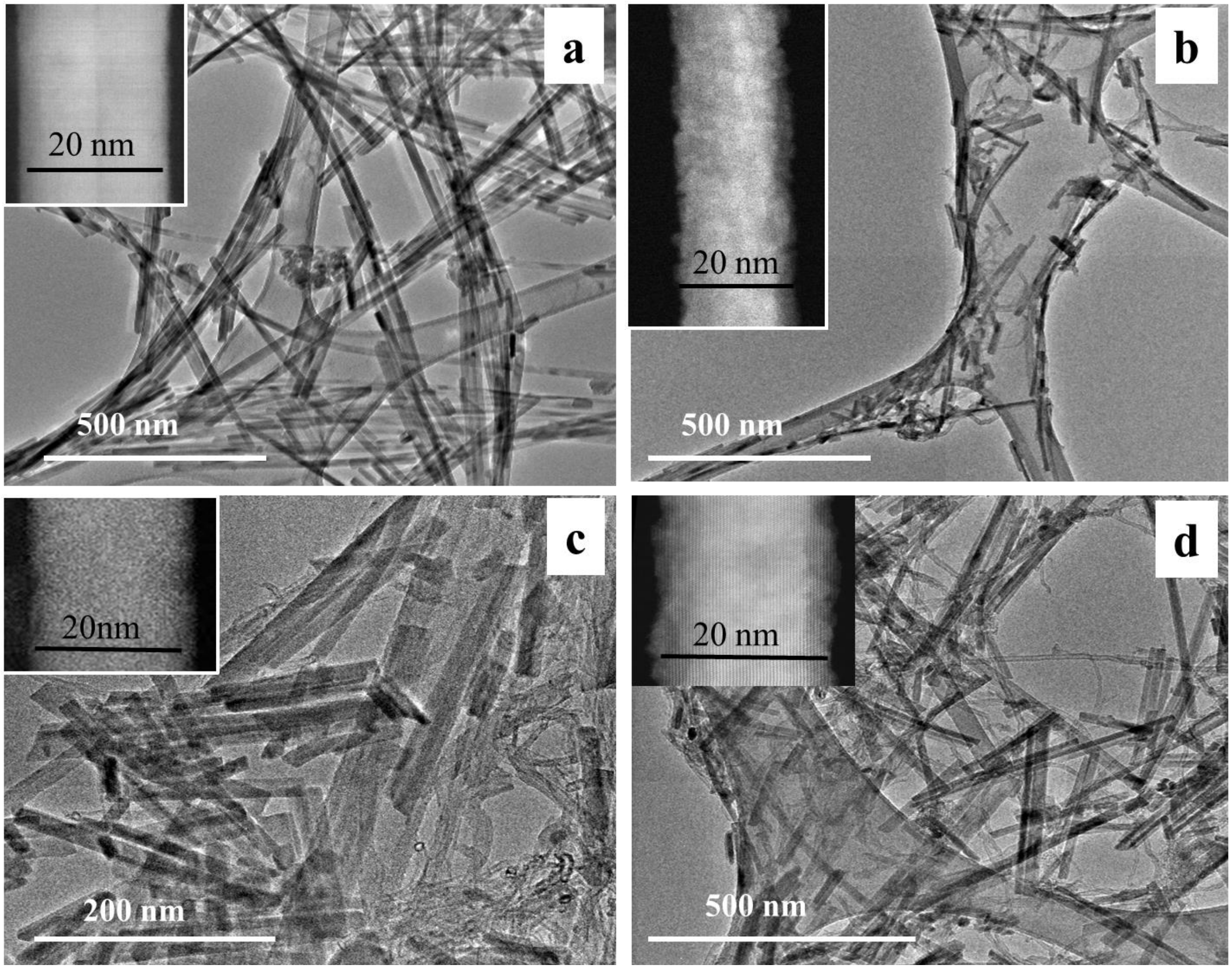

Fig. S7 Low-magnification STEM images showing size difference of the as-made, 100 cycled, 300 cycled and regenerated BFSSC. (**a**) The as-made BFSSC, (**b**) The BFSSC sample after 100 cycle, (**c**) the BFSSC sample after 300 cycles, and (**d**) the regenerated BFSSC sample. Scale bars are 500 nm. Insets are enlarged image of the corresponding nanorods (scale bars are 20 nm).

References:

1. T. Gao, M. Glerup, F. Krumeich, R. Nesper, H. Fjellvåg and P. Norby, *The Journal of Physical Chemistry C*, 2008, **112**, 13134-13140.

2. J. Luo, H. T. Zhu, H. M. Fan, J. K. Liang, H. L. Shi, G. H. Rao, J. B. Li, Z. M. Du and Z. X. Shen, *J. Phys. Chem. C*, 2008, **112**, 12594-12598.

3. J. Yuan, K. Laubernds, J. Villegas, S. Gomez and S. L. Suib, *Advanced Materials*, 2004, **16**, 1729-1732.

4. J. Yuan, W.-N. Li, S. Gomez and S. L. Suib, *Journal of the American Chemical Society*, 2005, **127**, 14184-14185.

5. K. Edström, T. Gustafsson and J. O. Thomas, *Electrochimica Acta*, 2004, **50**, 397-403.

6. W. J. Lee, K. Prasanna, Y. N. Jo, K. J. Kim, H. S. Kim and C. W. Lee, *Physical chemistry chemical physics : PCCP*, 2014, **16**, 17062-17071.

7. W. Yan, T. Ayvazian, J. Kim, Y. Liu, K. C. Donavan, W. Xing, Y. Yang, J. C. Hemminger and R. M. Penner, *ACS Nano*, 2011, **5**, 8275-8287.

8. C. Zhang, C. Feng, P. Zhang, Z. Guo, Z. Chen, S. Li and H. Liu, *RSC Adv.*, 2012, **2**, 1643-1649.

9. W. K. Pang, V. K. Peterson, N. Sharma, C. Zhang and Z. Guo, *The Journal of Physical Chemistry C*, 2014, **118**, 3976-3983.